Chain Unfolding in Single Crystals of Ultralong Alkane $C_{390}H_{782}$ and Polyethylene: An Atomic Force Microscopy Study

Sergei N. Magonov* and Natalya A. Yerina

Digital Instruments/Veeco Metrology Group, 112 Robin Hill Rd., Santa Barbara, California 93110

Goran Ungar

Department of Engineering Materials, University of Sheffield S1 3JD, U.K.

Darrell H. Reneker

Department of Polymer Science, University of Akron, Akron, Ohio 44325

Dimitri A. Ivanov

Laboratoire de Physique des Polymères, CP 223, Université Libre de Bruxelles, Boulevard du Triomphe, B-1050 Brussels, Belgium

Received February 24, 2003; Revised Manuscript Received May 9, 2003

ABSTRACT: Ultralong alkanes (C_nH_{2n+2}, $n > 150$) are generally considered as the most appropriate model for polyethylene, PE, and studies of these compounds can shed light on fine structural features of polymer crystals and the mechanisms of polymer crystallization. High-temperature atomic force microscopy was applied for comparative studies of solution-grown single crystals of $C_{390}H_{782}$ (the longest available alkane) and PE. While the structures of single crystals of $C_{390}H_{782}$ and PE are similar, the details of their thermal behavior are quite different. The structural transitions in $C_{390}H_{782}$ crystals follow the typical oligomer-type integral chain-folding scheme. Upon annealing, the alkane crystal undergoes a complete series of transformations corresponding to stepwise unfolding from the folded-in-five conformation toward the fully extended-chain crystal. The chain unfolding in PE crystals is a continuous and slower process. The morphological evolution of single crystals on heating is found to be dependent on the presence of solvent traces. Melting of the alkane crystals on graphite is accompanied by spreading of the alkane onto the substrate leading to the formation of a thin epitaxial layer. The complete melting of this film occurs at 185 °C, i.e., approximately 55 °C above the melting point of the bulk material.

Introduction

Crystallization of polymer molecules in dilute solution proceeds by multiple folding of individual chains into thin lamellae whose size and shape depend on crystallization conditions. The multiple chain folding in single polymer crystals was first suggested by Storks,[1] who presumed that "the macromolecules are folded back and forth upon themselves in such a way that adjacent sections remain parallel". This idea was further developed by Keller and colleagues.[2] For more than 40 years, single crystals of polyethylene (PE)[3] and their aggregates (mats) have been examined by various characterization techniques such as optical microscopy, electron microscopy, electron and X-ray diffraction (ED, SAXS, and WAXS), differential scanning calorimetry (DSC), and others. Upon crystallization in dilute solution, the single crystals of PE have the shape of a hollow pyramid. When deposited on a substrate, the hollow pyramid collapses to flat lozenge-shaped lamellae whose thickness (usually in the range of 10−20 nm) is determined by the length of a straight chain stem. The chain axis (*c* axis of the orthorhombic unit cell) is oriented at an angle >60° to the lamella surface. In TEM micrographs of PE crystals, there are central ridges along the *a* and *b* axes, which divide the crystal into sectors.[4] Four sectors are common for diamond-shaped crystals (4-sided hollow pyramids in solution) and six sectors for truncated diamonds (6-sided pyramids in solution). The crystal sectors differ in the tilt of the basal plane and in the orientation of chain folds. Pleats and fine surface texture of crystal sectors most likely reflect an incomplete structure relaxation following solvent removal and crystal flattening.[3,5]

Recently in situ studies were carried out on crystallization and morphology of long alkanes $C_{162}H_{326}$[6] and $C_{246}H_{494}$,[7] exploring the origin of the dependence of morphology on crystallization temperature.

Despite extensive research efforts, there are a number of open questions concerning the structure of polymer single crystals. One such question, addressing the mechanisms of lamellar thickening induced by thermal annealing of polymer materials**,** is of fundamental and practical importance. Previously, Reneker and Geil[8] suggested two alternative structural models of PE crystal, in which the folds in successive fold planes are aligned along {100}, {010} and the {110}, {130} planes, respectively. Methods such as mixed crystal infrared spectroscopy[9] and surface decoration (see later) have helped establish the approximate proportion of {110} and {100} folds in different morphologies. The thickness of the lamellae, one of the main characteristics of a crystalline polymer, strongly depends on crystallization temperature.[10−12] Thermal annealing promotes partial unfolding of polymer chains toward the more energetically favorable extended chain conformation. This process, i.e., lamellar thickening, has been previously examined with TEM and SAXS/WAXS. In TEM, the change in crystal thickness is estimated using oblique shadowing. Local electron diffraction or X-ray diffraction on single-crystal mats is applied for identification of the crystallographic axes and the chain tilt with respect to

10.1021/ma0301303 CCC: $25.00
Published on Web 06/25/2003

the lamellar basal plane. Measurements of the long period, i.e., a repeat distance in lamellar stacks, and crystal thickness are performed in SAXS studies of single-crystal mats.[13]

In their pioneering work,[10] Keller and O'Connor noticed that during annealing of PE crystals the initial spacing of 12 nm disappeared to give rise to a larger one (20−30 nm). Statton and Geil[12] found that the estimate of the crystal thickness based on TEM shadowing is consistent with SAXS long period determined in studies of single-crystal mats. They also observed the formation of holes in single PE crystals during annealing from which they deduced the occurrence of a refolding process.

Notwithstanding the general consistency of the results on partial chain unfolding during annealing, there has been disagreement between authors regarding reorientation of the molecular axis in PE sample. Thus, Bassett and Keller[11] indicated that annealing caused a rotation of the chain axis about *b* whereby the *a* axis became perpendicular to the lamellar surface and the *c* axis parallel to it. Contrary to this work, Statton and Geil reported[12] that the chain axis is oriented almost perpendicular to the single-crystal surface before and after heating to 125 °C. Geil[3] attributed this controversy to a possible effect of solvent retained in the samples studied by Bassett and Keller.

In addition to TEM studies, lamellar thickening has been examined with optical microscopy by Kovacs and co-workers[14] who observed spectacular thickening patterns (pathological crystals) for sharp fractions of poly(ethylene oxide), PEO. In recent years, studies of single polymer crystals have been extended owing to the availability of model compounds such as ultralong uniform alkanes,[15] as long as $C_{390}H_{782}$, and new characterization techniques such as atomic force microscopy (AFM). Studies on crystallization, morphology, lamellar thickening, etc., using model polymers, including monodisperse alkanes, nylons, PEO fractions, and others, have been reviewed recently.[16]

Studies on long alkanes have shown that chains consisting of a minimum of 120−150 carbon atoms are able to crystallize in a folded form. Importantly, the crystals of long alkanes exhibit integral chain folding. For example, depending on crystallization temperature, the $C_{390}H_{782}$ normal alkane can adopt conformations from fully extended to folded-in-five, F5.[17] DSC, TEM, and SAXS data revealed transitions between different folded forms as well as isothermal thickening of single crystals of long alkanes $C_{198}H_{398}$ and $C_{294}H_{590}$.[18−20] In contrast to polymers, crystals of ultralong alkanes grown in dilute solution could slowly thicken at the temperature of crystallization.[18] Isothermal thickening of $C_{198}H_{398}$ was shown to proceed from the once folded to extended chain crystal, and in the case of $C_{294}H_{590}$ crystals, its twice-folded form converts to once-folded, and its triple-folded form to twice-folded. Visualization of morphology of $C_{198}H_{398}$ crystals annealed in solution revealed that the thickening spreads along the sector boundaries. It was suggested that chain sliding along the (110) lattice plane allows material feed to the thickening regions. The thickening of $C_{294}H_{590}$ crystal proceeded differently, with a complete loss of crystal shape.

AFM technique, which is based on precise rastering of a sharp microscopic probe over the sample surface, offers high-resolution 3D profiling of surface structures. AFM applications to polymers[21] include visualization of single polymer macromolecules and nanometer-scale structures and also compositional mapping of semicrystalline polymers and heterogeneous polymer systems such as block copolymers and polymer blends. At present, AFM capabilities in analysis of polymers are further extended with imaging at elevated temperatures (up to 250 °C). This capability allows in situ monitoring of polymer structure changes during different thermal transitions[22] that has been illustrated in studies of PE recrystallization in ultrathin layers[23] and melt-crystallization of poly(ethylene terephthalate).[24]

Single crystals of PE were some of the first polymer objects examined with AFM.[25,26] AFM imaging complements TEM providing precise measurements of single-crystal height (lamellar thickness) and high-resolution visualization of lamellar surface structure. AFM images of lamellar surfaces of PE,[27] PEO,[28] and polysilane[29] exhibit periodic patterns reflecting molecular lattices of these crystals. Still it is not clear if these results gave an unambiguous answer to the question concerning the degree of order on the lamellar surface of single polymers crystals. Since these images were recorded at elevated tip-force (contact mode), penetration of the AFM probe through a less ordered top layer into subsurface crystal lattice could not be excluded. A gentler imaging (tapping mode) revealed tiny boundaries between the fold domains and the fine nanometer-scale texture of PE single crystals.[30] The latter is more likely to be related to the mode of surface assembly of poorly ordered material than to regular folds.

In this paper, we present results of a comparative AFM study of single crystals of ultralong alkane $C_{390}H_{782}$ and PE at different temperatures. Our initial intent was to visualize chain unfolding transitions, which accompany annealing of the crystals. Single crystals of $C_{390}H_{782}$ alkane (chains folded in five, thickness ∼10 nm) were chosen as the most appropriate model of a PE single crystal. Recent AFM studies of annealing of single crystals of $C_{162}H_{326}$[31] and PE[32] demonstrated that this method complements other characterization techniques in studies of the chain unfolding transitions. Particularly, it was shown that annealing of $C_{162}H_{326}$ single crystal at 90 °C induces several simultaneous processes, such as appearance of holes, dendritic growth at crystal edges, and thickening of nonmolten areas. Some of these processes are related to unfolding of once-folded chains. AFM images of lozenge-shaped single crystals of PE subjected to thermal annealing also revealed the formation of numerous holes[32] as a result of crystal thickening. The present work is an extension of AFM studies of lamellar thickening on single crystals of $C_{390}H_{782}$ alkane and PE with different preparation history.

For the first time, thermal behavior of crystals of the longest alkane $C_{390}H_{782}$ has been studied in direct space with high resolution and compared with that of PE. Fine-scale surface features of $C_{390}H_{782}$ crystals closely resemble those of PE crystals. It was found that striking differences characterize the morphological evolution during annealing of the alkane and PE crystals with different preparation history, which points to an important role of solvent traces in these processes. Novel observations of epitaxial order of alkane layers on graphite (i.e., the layers lying immediately on the substrate) and their stability at elevated temperatures (up to 180 °C) are also reported.

Experimental Part

Materials. In this study we used the ultralong alkane $C_{390}H_{782}$ kindly provided by Dr. G. M. Brooke.[15] Single crystals of $C_{390}H_{782}$ were prepared by spreading a droplet of a hot alkane solution in xylene (1 mg/mL) on a flat substrate (graphite, Si) with a spin-coater (Speedline Technologies model P6204) at 2000 rpm. Crystals with lozenge shape were found in spin-cast samples of $C_{390}H_{782}$ and $C_{242}H_{486}$. Here we report the data obtained for $C_{390}H_{782}$ alkane only; the results of AFM studies of $C_{242}H_{486}$ crystals will be published elsewhere.[33]

Single crystals of PE were prepared by the self-seeding technique[34] from a standard material (NBS 1475, M_w ~50K) at 70 °C.[25] The material was dissolved in 20 milliliters of xylene by heating at temperatures just below the boiling point of xylene. The solution was cooled to room temperature in a few minutes, during which time dendritic crystals grew. The suspension of crystals in the solvent was reheated slowly at the rate of about 1 °C/min. Heating stopped when the solution became transparent, as judged by eye, near 96 °C. Experience shows that at this point most of the polymer is dissolved, but that many nuclei, too small to scatter light, remain. The solution was then cooled at an initial rate of around 12 °C/min, which decreased to 6 °C/min after 2 min. The temperature continued to drop at ever-slower rates until room temperature. Visual observation of the light scattering showed little change at temperatures below 80 °C. Many small crystals of the sort shown below grew from the nuclei. The crystals remained in suspension in the xylene and were stored at room temperature. For the purpose of our study, the crystals of the alkane and PE precipitated from solutions on a substrate were dried either at ambient conditions for several weeks or in a vacuum at 70 °C for 3 days. The latter crystals are called "dry", whereas those dried at ambient conditions are referred to as "wet".

Methods. After preparation, the alkane and PE single crystals deposited on substrates were preliminary examined with a differential interference contrast optical microscope (Nikon Eclipse ME600). AFM studies were performed with commercial scanning probe microscopes Nanoscope IIIA and IV MultiMode (Digital Instruments) equipped with a heating accessory. In this accessory, a dual heating of the sample and probe is performed to ensure the conditions of thermal equilibrium in the tip−sample contact area. Imaging at elevated temperatures (up to 200 °C) was conducted in a He atmosphere to prevent the sample oxidation. In some cases, after imaging at high temperature the sample was cooled to room temperature and imaging was repeated. This made it possible to improve the image quality due to the increased stiffness of the sample. Other details concerning the heating accessory and AFM studies at elevated temperatures can be found elsewhere.[24,35] Etched Si probes with force constants of 1−3 and 40−50 N/m were used in the experiments. Lateral calibration of the piezoelectric scanner applied in this study was checked by measuring the 7.5 nm lamellar spacing of $C_{60}H_{122}$ epitaxial layers on graphite.[36] The vertical calibration was verified by using 24 nm steps of a commercial calibration standard (MikroMasch).

AFM images of the alkane and PE crystals were analyzed using bearing ratio and power spectral density computed with the help of the Nanoscope software as well as with a home-built software.[37] Morphological parameters of semicrystalline structures have been evaluated from AFM images using the classical one-dimensional correlation function approach[38,39] used to interpret SAXS data. To this end, the images were first converted to the binary form in which the image pixels were ascribed either to the crystalline lamellae or the background based on automatic analysis of the objects shape. In the second stage, the two-dimensional power spectral density function ($P_2(s)$) was computed from the binary images ($u(r)$) up to the critical, or Nyquist, frequency as follows:

$$P_2(s) = \frac{1}{A}\left|\int u(r)W(r)\exp(2\pi i s r)\,\mathrm{d}^2 r\right|^2 \qquad (1)$$

A, $W(r)$, and s denote the image surface area, a window function,[40] and the two-dimensional reciprocal space vector, respectively. The $P_2(s)$ function was further converted to its one-dimensional form by performing circular averaging:

$$P_1(s) = \frac{1}{2\pi s}\int P_2(s')\delta(|s'| - s)\,\mathrm{d}^2 s' \qquad (2)$$

The SAXS-type one-dimensional correlation function $\gamma(l)_{AFM}$ was calculated as the real part of the Fourier transform of $P_1(s)$ corrected for Lorentz:

$$\gamma(l)_{AFM} = \mathrm{Re}\left[\int P_1(s)\exp(2\pi i s l)s\,\mathrm{d}s\right] \qquad (3)$$

The crystal and amorphous layer thicknesses, L_c and L_a, were calculated using the standard relationship:

$$L_c = \frac{L_B \pm \sqrt{{L_B}^2 - 4L_B r_0}}{2} \qquad (4)$$

In eq 4 L_B stands for the long period ($L_B \equiv L_c + L_a$) determined from the first subsidiary maximum of $\gamma(l)$, and r_o corresponds to the smallest positive root of the equation $\gamma(l) = 0$. The sign in the numerator of the right-hand side of eq 4 depends on whether the crystals are thinner or thicker than the amorphous intercrystalline layers, i.e., whether the linear crystallinity $\varphi_{c,lin}$ ($\varphi_{c,lin} \equiv (L_c/L_B)$) is lower or higher than 0.5.

Results

Imaging of As-Prepared "Wet" $C_{390}H_{782}$ Crystals. The optical micrograph of $C_{390}H_{782}$ adsorbates in Figure 1a shows a number of lozenge-shaped crystals with lateral dimensions of about 10 μm. The crystal in the center of the micrograph displays a pleat along its short diagonal. This is similar to TEM observations on single crystals of PE[3] where such pleats were found to be parallel to the b axis. This resemblance becomes even more evident when fine morphological details of the alkane single crystals are inspected in AFM images (Figure 1b−d). Two "wet" $C_{390}H_{782}$ crystals lying on top of each other are seen in the height image in Figure 1b. The cross-section profile indicates that the thickness of the crystals is 9.5 nm. This value correlates well with

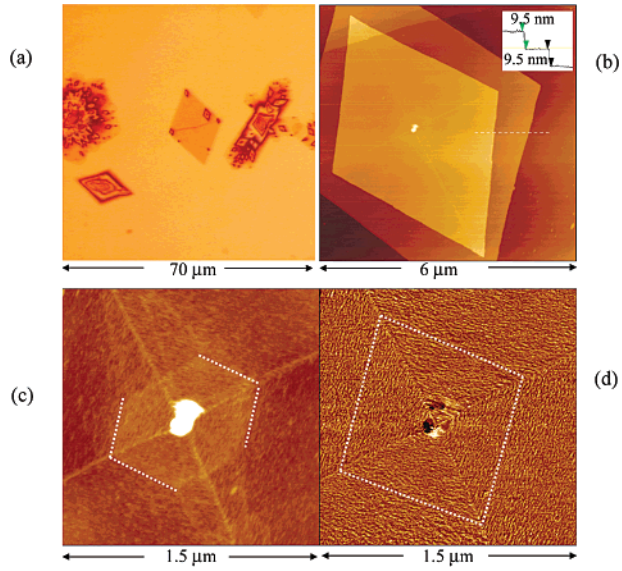

Figure 1. (a) Optical micrograph of $C_{390}H_{782}$ adsorbate prepared by spin-coating a dilute solution in hot xylene on graphite. (b−d) Ambient temperature AFM images of two "wet" $C_{390}H_{782}$ single crystals on graphite: (b, c) height and (d) phase images. The inset in part b displays a cross-section profile measured along the white dotted line.

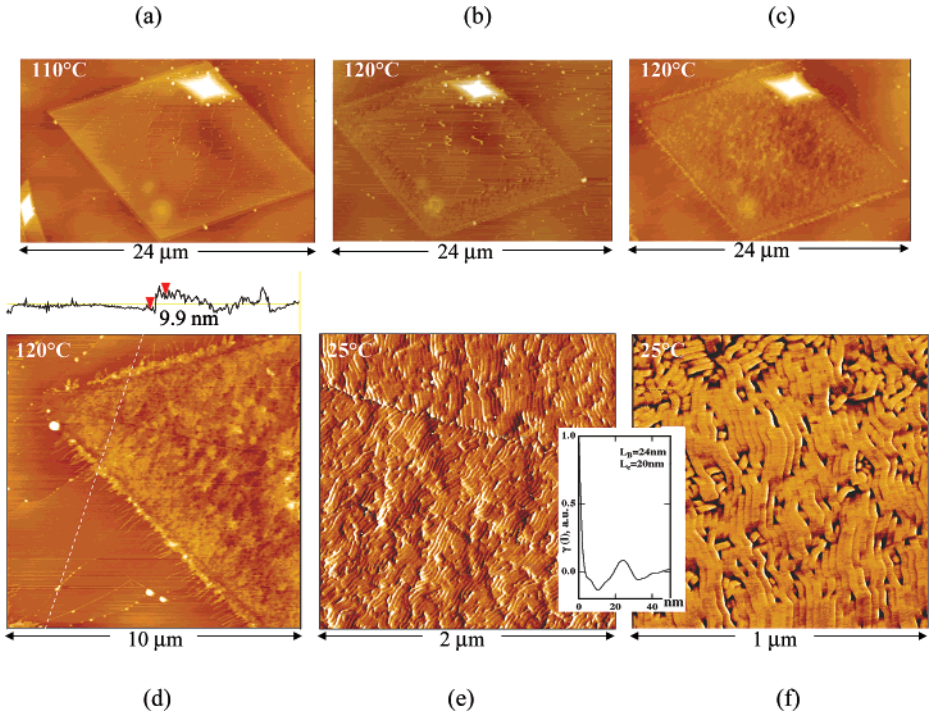

Figure 2. (a−c) Height images of a "wet" $C_{390}H_{782}$ crystal measured at different temperatures. Images in parts b and c are recorded with a 10 min interval at 120 °C. (d) Height image of a corner of the crystal shown in parts a−c. Cross-section profile taken along the white dotted line is given above the image. (e−f) Phase images of a part of the crystal corner in part d. One-dimensional correlation function computed from the image in part f is given in the insert between the images.

the stem length of the F5 conformation of the $C_{390}H_{782}$ chain (49.7/5 = 9.9 nm). Therefore, it is likely that the alkane chains are oriented normal or nearly normal to the single-crystal surface. SAXS data on $C_{390}H_{782}$ crystals grown from bulk solution under similar conditions give a long period of exactly 9.9 nm.[16,17] Thin bright lines running along the crystal diagonals are seen on the top surface of the crystal (Figure 1b). These features are emphasized in the high-resolution height image in Figure 1c. The lines and ridges define four (110) sectors of this crystal similar to those of solution-grown single crystals of PE after deposition on a flat substrate. An elevated crystal nucleus surrounded by a distorted hexagonal pattern is seen in the center of the crystal. The edges of this hexagon are marked with white dotted lines. The presence of this hexagon might indicate that the crystal growth started at a somewhat higher temperature where similar to single crystals of PE[11] and alkanes $C_{162}H_{326}$ and $C_{246}H_{494}$,[6,7] the $C_{390}H_{782}$ crystal could have grown with a truncated lozenge shape. Indeed, we have two additional (100) faces. The phase image of the same location (Figure 1d) shows a fine surface texture of the sectors composed of nanometer-scale surface corrugations barely seen in the height image. The orientation of these corrugations are nearly orthogonal in adjacent sectors (marked by dotted lines), which is close to that of the much coarser pleats aligned parallel to (530) or (310) planes in single crystals of PE deposited on a substrate.[8] We suppose that these surface features, also referred to as wrinkles, originate from crystal flattening on the substrate.

Imaging of "Wet" $C_{390}H_{782}$ Single Crystal after Thermal Annealing. Case 1. Heating of "wet" $C_{390}H_{782}$ crystals was accompanied by morphological modifications revealed by AFM height and phase images in Figures 2a−f. The crystal in Figure 2a, which was imaged after heating to 110 °C, shows no change in shape or appearance as compared to its initial state. The only changes observed were in the positions of the small grains and short fibrilar features, which might be assigned to noncrystallized material precipitated from remnants of solution on the crystal surface. Transformation of surface morphology was noticed after heating the crystal to 120 °C. Coarsening of the top surface started at the crystal edges and advanced toward the center (Figure 2b,c). The sector boundaries, which were not visible before, became distinguishable. A closer view of one of the crystal corners in Figure 2d highlights these morphological changes: an elevated strip of material along the crystal perimeter is adjoined from the outside by straight fibrils spreading onto the graphite, and from the inner side by a darker strip. This height corrugation might be related to crystal thickening, which commonly starts at crystal edges.[18,20,31] Numerous dark patches of different size are seen at various locations on the crystal surface. A cross-section profile taken along the dotted line shows that these height corrugations are comparable to the crystal thickness. Apparently, major structural rearrangements have occurred during the annealing.

The most drastic changes are recognized in the phase images at smaller scan sizes (Figure 2e,f**,** the crystal nucleus is to the right of these areas), which reveal the fine structure that appeared during heating of the "wet" $C_{390}H_{782}$ crystal. As a result of the annealing, the chevronlike pattern is formed by numerous wavy structures. These slightly wavy structures can be tentatively assigned to edge-on lamellae,[41] yet their third (i.e., vertical) dimension is unknown. It can be seen that the edge-on lamellae, or ribbons, are differently oriented in the neighboring sectors. They are aligned perpendicular to the crystal edges and form an angle of ∼60° with the sector boundary (Figure 2e). According to the quantitative analysis of the AFM image in Figure 2f performed

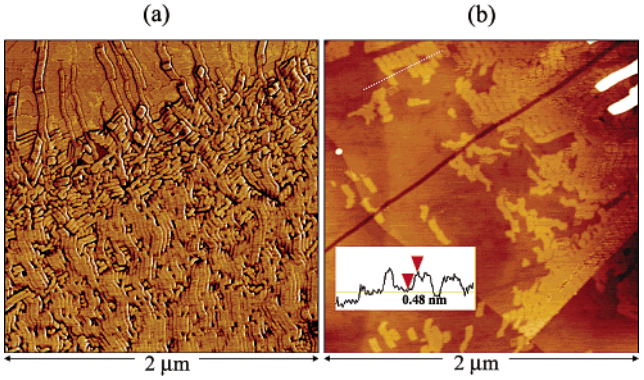

Figure 3. (a) Phase image of the edge of the "wet" $C_{390}H_{782}$ crystal after heating to 120 °C. (b) Height image of a region on graphite located close to the $C_{390}H_{782}$ crystal after thermal treatment at 120 °C. Bright strips at the upper right corner of the image show two wide lamellae ($C_{390}H_{782}$ chains in E conformation). The insert shows a cross-section profile along the direction indicated with a white dotted line.

with the help of the one-dimensional correlation function, the width of individual ribbons is approximately 20 nm and the repeat distance in their stacks is 24 nm. Thus, linear crystallinity in the lamellar stacks is ~80%.[42] The size of the ribbons suggests the F2 (once-folded) chain conformation with chains being oriented parallel to the surface of the original lamellae. Therefore, annealing of wet $C_{390}H_{782}$ crystals resulted in chain unfolding and reorientation by 90°. A possible origin of the chevronlike arrangement of the lamellar ribbons is discussed below.

It is important to understand the nature of morphological changes produced during annealing of "wet" $C_{390}H_{782}$ crystals. On the basis of the high degree of ordering of the ribbons normal to the sector growth face, we suggest that they had grown through local melting of the "wet" crystal and epitaxial recrystallization edge-on and normal to the direction of the underlying folds. Indeed, the ribbon orientation in different sectors is similar to that observed in epitaxial decoration of PE single crystals with $C_{36}H_{74}$, where the $C_{36}H_{74}$ chains were also aligned along the PE fold planes.[43] The highly uneven surface of the annealed crystal visible in the height images, where height variations are comparable with the crystal thickness, is in favor of our suggestion. Other indirect evidence comes from our recent data obtained on annealing of "wet" $C_{242}H_{486}$ crystals, where a stepwise annealing from 100 to 120 °C was accompanied by growth of edge-on lamellae and an increase of crystallinity.[33]

The chain unfolding occurs somewhat differently at the edge of the $C_{390}H_{782}$ crystal and in the nearby substrate region (Figure 3a,b). The phase image in Figure 3a demonstrates that the edge-on lamellae with F2 chain conformation are aligned parallel to the crystal edge close to the border inside the initial crystal boundary. However where the lamellae spread onto the graphite surface they align perpendicular to the edge. In the top left corner of this image, one sees several individual lamellae extended from the crystal border to the substrate. Some are formed by a merger of two F2 lamellae to form thicker ones, which are 44−45 nm in width. In a few double-lamellae, a border between the neighbors is practically eliminated. This suggests the unfolding of $C_{390}H_{782}$ chains to the fully extended conformation, (E-conformation). The fact that the lamellar width is slightly smaller than the size of a fully extended $C_{390}H_{782}$ chain (49.7 nm) suggests that the alkane chains are tilted with respect to the normal to the lamellae border. Between these wide lamellae and further away from the crystal, there is a thin layer of $C_{390}H_{782}$ alkane, which is best resolved in the height image in Figure 3b. This image shows stacks of ribbons (bright areas) with different orientations that might have been induced by the substrate. The lamellae-free areas (darker) are most likely covered with a thin layer of a disordered material, which smoothens graphite imperfections such as steps and cracks. The individual ribbons are 46−47 nm wide and only 0.48 nm high, as measured from the cross-section profile shown in Figure 3b. These data imply that the ribbons are likely to be composed of a single-layer of the alkane chains.

Imaging of "Wet" $C_{390}H_{782}$ Single Crystal after Thermal Annealing. Case 2. To extend our observations of chain unfolding during annealing of "wet" $C_{390}H_{782}$ crystals, we describe the morphological evolution of two overlaying crystals shown in Figure 4a during heating to 120 and 130 °C. The height profile shows that the height of each of the crystals is ~9.4 nm, which is in agreement with the F5 chain conformation. The crystal whose long diagonal runs from the bottom right to the top left of the image lies on the top of the other crystal. This conclusion is based on the assumption that two spiral overgrowths at the obtuse apexes and a ridge in the center belong to the top crystal. It is interesting to note that the collapse of the top crystal resulted in steps of ~9.4 nm in height along the edges of the underlying one (these edges are indicated with two white arrows.) This happened due to the sliding of parts of the overlying crystal down to the substrate. Such process is facilitated by the fact that the alkane chains inside the crystals can slide along each other in the *c* axis direction. The same happens in PE crystals.[30]

Heating these crystals to 120 °C leads to roughening of the crystal center, yet the central pleat remains (Figure 4b). As in the case of the crystals shown in Figure 2a−c, the surface corrugations of the top crystal in Figure 4b (cf. the height profile (b) on the right) are comparable to the crystal thickness. It is clear that such roughening is caused by substantial structural change. Darker strips, which are seen at the left and right edges of this aggregate, are formed due to material transfer from these locations to the nearby thin bright strips (Figure 4b) and further into lamella "off-springs" onto the substrate (Figure 4c). Annealing at 130 °C intensifies the roughening of the crystal surface (Figure 4c). The cross-section profile in Figure 4c shows that crystal thickness became smaller. A closer view of the boxed area in Figure 4b is given in the phase image in Figure 4d. This image indicates that after heating to 120 °C, the chevronlike arrangement of ribbons on the crystal surface is similar to the one seen in Figure 2e,f. Indeed, within a sector, the ribbons are generally aligned perpendicular to the crystal edge. The corresponding power spectral density plot reveals a periodicity of 24 nm in lamellar stacking. This is in agreement with F2 conformation of the alkane chains. After heating to 130 °C, the chain unfolding continues (Figure 4e). Thus, the power spectral density of this image, which includes the crystal edge and the nearby substrate region covered by a monomolecular layer of the spread alkane (Figure 4e), shows that the layer spacing is in the 41−48 nm range. Consequently, the 130 °C annealing generates extended-chain lamellae, some of them probably com-

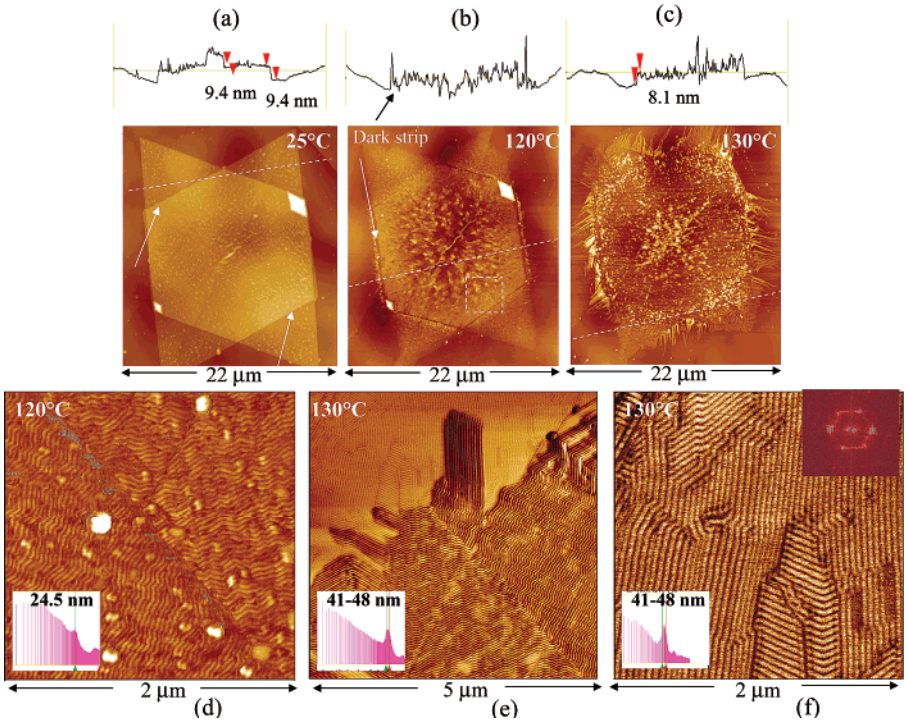

Figure 4. (a−c) Height images of two wet crystals of $C_{390}H_{782}$ measured at different temperatures. Cross-section profiles along the directions indicated with white dotted lines in parts a−c are given on the top. (d) Phase image of an area (white rectangle) in the bottom corner of the overlaying crystal in part b. (e) Phase image of a location in the middle of the crystal edge shown in part c. (f) Phase image corresponding to the top left corner of part e. Insets in parts e and f show the corresponding spectral power plots. The insert in the top right corner of part f shows a 2D power spectral density plot.

posed of tilted chains. A part of the substrate covered by $C_{390}H_{782}$ ribbons is enlarged in the phase image in Figure 4f. The ribbons are aligned in three main directions, which differs by ∼60°, and this is confirmed by the two-dimensional power spectrum, which shows an overall hexagonal ordering (nonequivalent intensities of the spots reflect a different number of ribbons aligned along the preferential directions). This arrangement is consistent with the epitaxial order of the alkane chains on graphite. The two-dimensional power spectrum shows a hexagonal ordering that might be identified with the epitaxial order of the alkane chains on graphite. The origin of local defects such as linear dislocations, kinks and others seen in the image in Figure 4f can be explained taking into account possible changes in lamellar orientation caused by chain tilt inside the ribbons and its dependence on temperature.[20,44]

Epitaxial Layers of $C_{390}H_{782}$ on Graphite. In our initial attempts to study lamellar ordering on graphite at different temperatures, we performed AFM experiments on $C_{390}H_{782}$ at even higher temperatures, up to 190 °C. This was motivated by the literature data on unusually high thermal stability of adsorbed monolayers,[45] and also by our recent findings that epitaxial layers of $C_{60}H_{122}$ on graphite are stable at temperatures up to 50 °C above the bulk melting point.[36] The images in Figure 5, parts a−d show the alkane layer at 160 and 170 °C. This layer was found at the location where the single crystal of $C_{390}H_{782}$ had melted at 130 °C. A parquetlike morphology of the $C_{390}H_{782}$ ribbons observed at 160 °C (Figure 5a,b) is similar to the one in Figure 4f. It shows a clear hexagonal pattern in reciprocal space (cf. the 2D power spectrum at the left of Figure 5b). Also, as in the previous case, the periodicity of the structure is ∼43 nm, which is smaller than 49.7 nm—the length of a completely extended $C_{390}H_{782}$ chain. This indicates that the chains could be tilted by about 30° with respect to the ribbon normal, i.e., close to the usual 35° tilt angle found in long alkanes[20] and PE[46] close to the melting temperature. The images of the same location at 170 °C (Figure 5c,d) show strikingly different morphology consisting of two domains with linear strips of ∼48 nm in width. We assume that these changes are caused by a structural transition, occurring between 160 and 170 °C, which involves rearrangement of the alkane chains from inclined to almost perpendicular to the ribbon edges. This new morphology was observed also at 180 °C. Yet imaging at 190 °C did not reveal any ordered structures, most likely due to a complete melting of this layer. A more detailed description of the lamellar ordering of single $C_{390}H_{782}$ and $C_{242}H_{486}$ layers on graphite and their temperature behavior will be given elsewhere.[44,33]

Imaging of Dry $C_{390}H_{782}$ Crystals upon Thermal Annealing. Imaging of $C_{390}H_{782}$ crystals, which have been dried in a vacuum, shows a different morphological pathway of the alkane chain unfolding. It includes thickening of crystals in the direction normal to the substrate and a formation of holes in nearby regions. A sequence of AFM images of the alkane crystal, recorded at 90 °C, is collected in Figure 6a−e. The first image, obtained after heating the sample to this temperature, shows a lozenge-shaped crystal with only minor changes compared to the same crystal at room temperature. Several parallel pleats and a sector boundary are seen on the surface of this crystal. Tiny dark spots corresponding to holes or circular dimples and slightly elevated regions start to appear along the crystal edges after tens of minutes' annealing time at 90 °C (Figure 6b). The recessed locations, growing in number and size, spread toward the crystal center forming a regular "framework" pattern (Figure 6d,e).

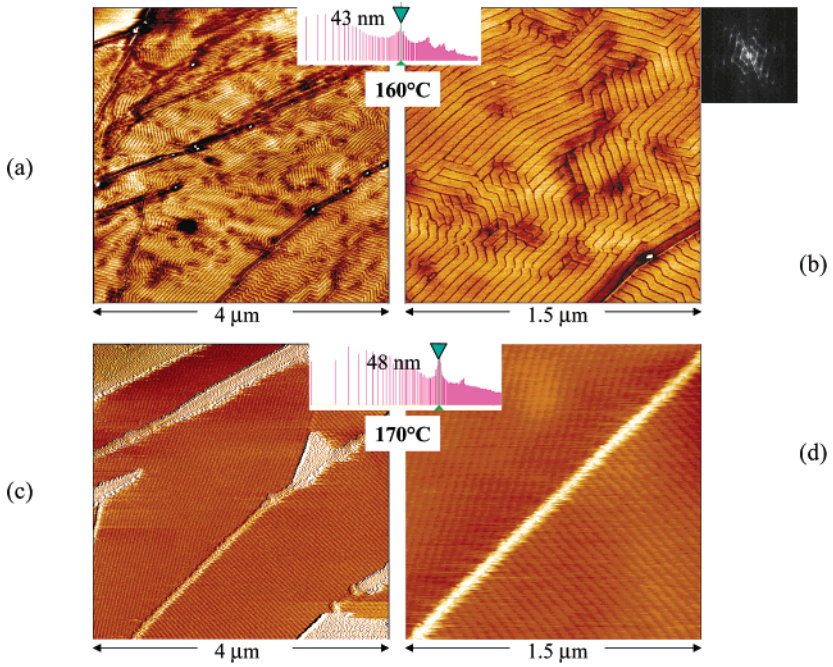

Figure 5. (a−d) Phase images of an epitaxial layer of $C_{390}H_{782}$ on graphite, which were recorded at different temperatures at the same location. Images in (b) and (d) are detailed views of locations inside parts a and c. The 2D power spectral density corresponding to the image in part b is shown on the right.

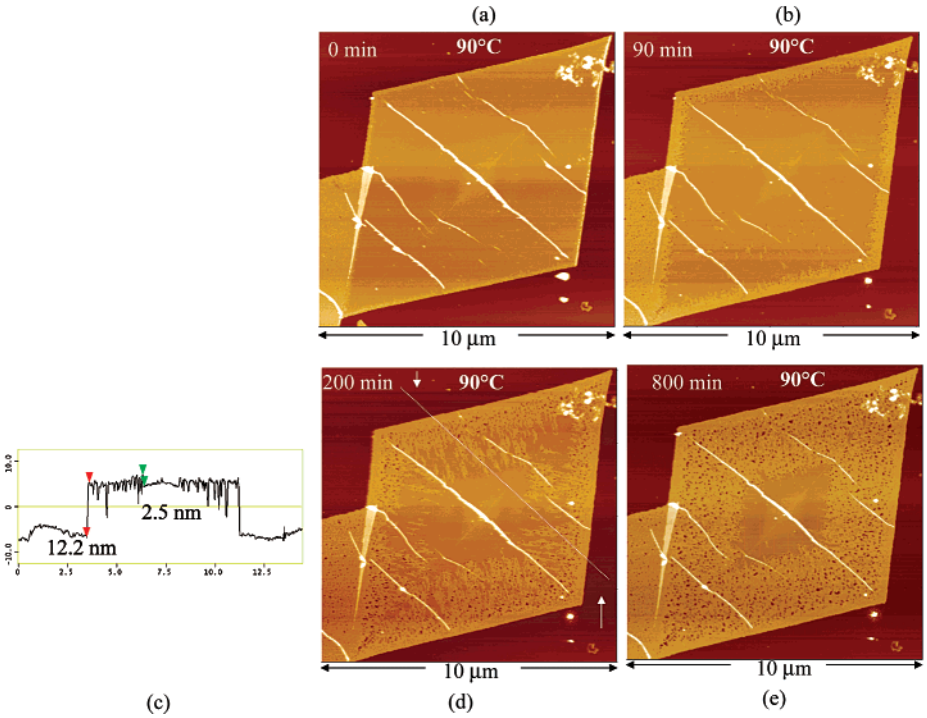

Figure 6. (a, b, d, e) Height images of a dry $C_{390}H_{782}$ crystal deposited on Si obtained in the course of annealing at 90 °C. (c) Cross-section profile measured along the dotted line in part d.

The cross-section profile in Figure 6c shows that crystal thickening results in 2.5 nm elevations on top of the original 9.7 nm thickness. This increase can be explained by unfolding of the alkane chain from the F5 to the F4 conformation. High-resolution images in Figure 7a,b show fine features of the developed morphology. Brighter rims surrounding numerous dimples and holes of different size are seen in Figure 7a. The corresponding cross-section profiles indicate that some of the rims are ∼0.2−0.3 nm in height. A part of the thickening front is shown in Figure 7b where many holes and dimples exhibit an elongated shape oriented toward the crystal center. In the profile traced across several holes and elevations, one finds not only the dominant 2.5 nm steps but also, similar to Figure 7a, numerous height variations in the 0.3−0.5 nm range (e.g., the feature in the profile above Figure 7b located immediately to the right of the 2.5 nm step indicated by arrows). Therefore, it is assumed that the elementary step of the unfolding process includes vertical sliding of the alkane chain on the scale of a single lattice parameter **c**.

In monitoring the crystal thickening process at higher temperatures, Figure 8a−f, it is convenient to use not

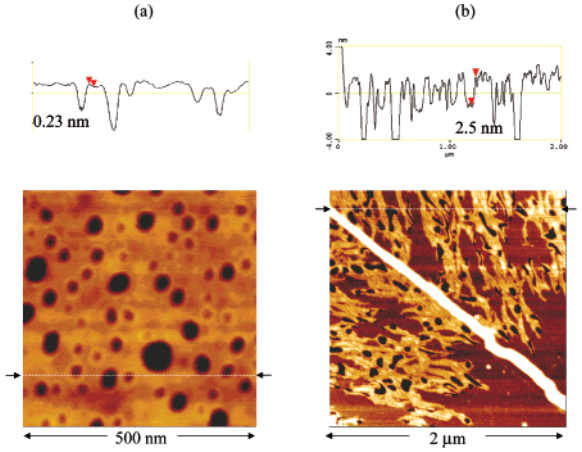

Figure 7. (a, b) High-resolution images of a dry $C_{390}H_{782}$ single-crystal annealed at 90 °C. (a) Detailed view of a thickened part of the crystal in which small local depressions are surrounded by rims of thickened material. (b) View of the propagation front corresponding to the thickening process. The cross sections measured along the dotted lines in parts a and b are given above the images. It can be seen that while the predominant height increase is about 2.5 nm (b), the very beginning of thickening results in local depressions (a) with a depth comparable to the lattice parameter *c*.

only the cross-section plots but also the height histograms that, in many instances, provide more statistically significant measurements of surface elevations. For example, it can be seen that steps (9.7 and 12 nm) corresponding to the F5 and F4 conformations dominate in the image recorded at 95 °C. This is clearly seen in the height histogram shown in the insert in the top left corner of Figure 8a. Annealing the crystal at 100 °C leads to the appearance and growth of a ∼ 15 nm thick crystalline layer (Figure 8b,c). This increase in thickness can be assigned to the alkane unfolding to the F3 conformation. During the annealing most of the surface dimples develop into holes, which increase in diameter resulting in the "Swiss cheese" morphology. Further on, major changes have been noticed at 120 °C, when the crystal disintegrates into islands (Figure 8d). The profile taken across the islands shows that many of them are 22−24 nm thick. We attribute this to chain unfolding to the next, i.e., the F2, conformation. The shortfall in crystal thickness with respect to the calculated half chain length of 25 nm is most likely due to the presence of chain tilt. The change from the perpendicular to the tilted chain structure at elevated temperatures would be in general agreement with the behavior of solution-crystallized short,[47] medium[48] and long alkanes.[20] Moreover, in a SAXS heating experiment on the single-crystal mat of $C_{390}H_{782}$ an F5 → F4 → F3 → F2 sequence of transformations was observed, where the initial F5 crystals were composed of perpendicularly oriented chains while the final F2 crystals were characterized by tilted chains (ref 11, Figure 49).

The thickness of the islands in the height image recorded at 130 °C (Figure 8e) approaches the length of the extended $C_{390}H_{782}$ chain. The estimation of the chain tilt with respect to the substrate normal gives ca. 20°, which is in line with the above discussion. In addition, one can see some structural features that have not been observed at lower temperatures. These are arrays of straight lines with a repeat distance of ∼ 44 nm (Figure 8f). We speculate that, similar to the structures in Figure 4d−f, these new surface features can be assigned either to thin ribbons of the extended-chain alkane decorating the underlying crystals, or to the recrystallized material that forms epitaxially aligned lamellar crystals. The latter assumption signifies that recrystallization of dry $C_{390}H_{782}$ crystals occurs at 130 °C which is higher than 120 °C, the recrystallization temperature observed for wet $C_{390}H_{782}$ crystals.

Imaging of Single Crystals of PE. "Wet" Crystal. We have thus demonstrated that morphological evolution accompanying heating of $C_{390}H_{782}$ crystals strongly depends on the presence of solvent traces. Here we describe the results of AFM observations of morphological changes in wet and dry PE crystals.

The "wet" single crystal of PE in Figure 9a exhibits a slightly truncated lozenge shape with a number of pleats oriented along the *b* axis. Although it was difficult to avoid the presence of some extraneous particles, probably due to adsorption of polymer on the crystal surface, several fine features are noticeable on a flat part of the crystal. They include a sector boundary along the *b* axis and a slightly darker frame at the crystal borders, which are better resolved in the image at 90 °C, Figure 9c. The height histogram shows that this crystal is ∼12 nm in height. Morphological changes have been observed after heating the crystal to 105 °C (Figure 9b). Although the crystal height (12.6 nm) did not change much after annealing at 105 °C, the crystal surface became covered with a number of holes and dimples. A more detailed view of this modified morphology can be seen in the high-magnification images of the boxed areas in Figure 9a,b. At temperatures below 105 °C, only the sector boundary and grainy top surface can be distinguished (Figure 9c). The surface texture becomes different at 105 °C, and numerous linear structures appear all over the surface (Figure 9d). After cooling to room temperature, this surface morphology is well resolved and can be assigned to stacks of edge-on lamellae (Figure 9e). Therefore, the annealing of a "wet" PE crystal had induced a lamellar rearrangement similar to one observed for "wet" $C_{390}H_{782}$ crystals. The lamellar orientations in the different sectors of the annealed PE crystal are generally perpendicular to the crystal faces. However, this orientation pattern is less defined than that in "wet" $C_{390}H_{782}$ crystals.

The correlation function analysis shows that interlamellar distance, or long period (L_B), is approximately 29 nm, whereas the thickness of the crystalline part of the lamellae, L_c, is ∼17 nm. This indicates partial unfolding of the PE chains, that initially had a stem length of ∼12 nm. Crystallinity of single PE crystals is high (∼85%),[42] whereas after annealing, a substantial difference between L_B and L_c gives linear crystallinity of only ∼59%.

Imaging of Single Crystals of PE. Dry Crystal. A dry PE crystal with a truncated lozenge shape was selected for annealing experiments. Heating of this crystal to 110 °C did not induce any changes in its morphology, which is characterized by a central pleat, a sector boundary along the short diagonal, a set of parallel wrinkles inside the smaller (200) sector and several spiral overgrowths (Figure 10a). The height of this crystal (∼12.4 nm) also remains the same as at room temperature. A sequence of AFM images of the PE crystal recorded during annealing at different temperatures is presented in Figure 11a−f. The morphological evolution, which started at 115 °C, proceeded via the formation of the hole morphology. There is evident lining-up of holes parallel to one of the [110] directions,

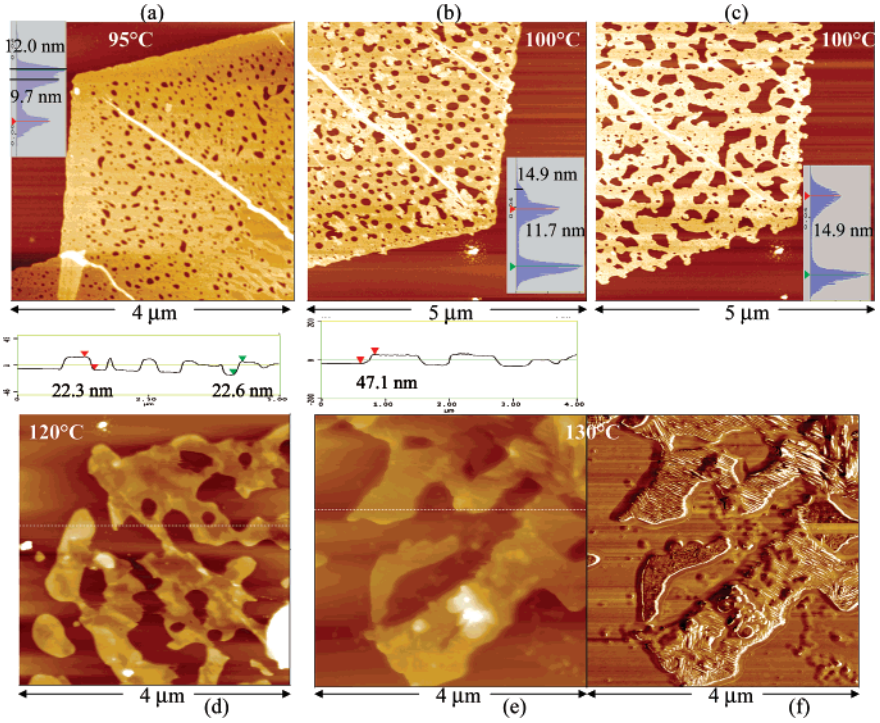

Figure 8. (a−d) Height images of a part of a dry $C_{390}H_{782}$ crystal measured at different temperatures. Insets in parts a−c show the corresponding height histograms in which the peaks of bimodal distributions represent the heights of the substrate and of the crystal surface. Numbers in the insets correspond to height differences between the cursors. (e, f) Height and phase images of remaining islands of the $C_{390}H_{782}$ crystal at 130 °C. The cross-section profiles above the images in parts d and e are measured along the white dotted lines.

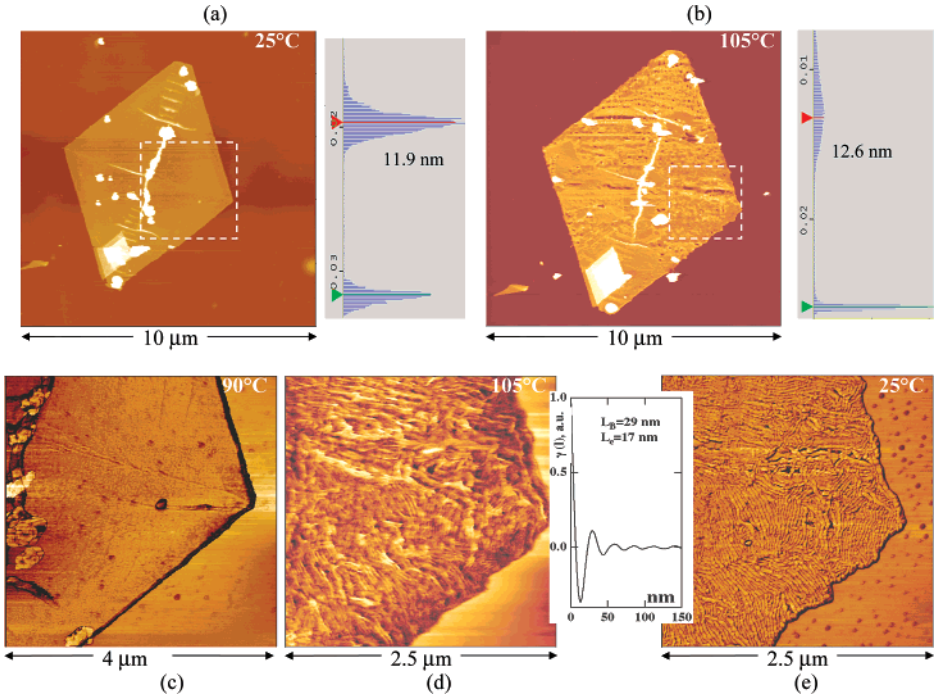

Figure 9. (a−e) AFM images of a "wet" single crystal of PE on Si substrate. (a, b) Height images taken at 25 and 105 °C. Height histograms are shown on the right of the images. (c−e) Phase images of a boxed area in part a, measured at 90, 105 and 25 °C, respectively. The SAXS-type one-dimensional correlation function corresponding to the image in part e is inserted between parts d and e.

but not along the other. Thus, in two sectors the rows of holes are normal to the growth face but in the other two they are definitely not. This lining-up might be related to residual stresses in the crystal originated during its collapse on the substrate. The holes appeared close to the crystal edges and propagated toward the crystal center. The high-resolution phase image in Figure 11d shows the advancing holes filling the surface of the spiral overgrowth and a part of the crystal edge. A cross-section profile (insert in Figure 11c) indicates that the thickened regions are up to 5 nm thicker than the original crystal. Surprisingly, the thickened regions surrounding the holes become noticeable only some time after the formation of the holes. This is evident from

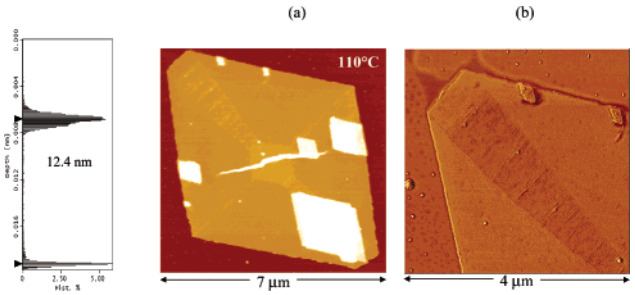

Figure 10. (a) Height image of a dry PE crystal on Si substrate at 110 °C. Height histogram is given on the left. Numbers in the insets correspond to height differences between the cursors, which indicate the height levels of the substrate and the top crystal surface. (b) Phase image of a part of the crystal shown in part a.

the comparison of the images in Figure 11a−c successively recorded at 115 °C at 10 min intervals. The dark holes, which are seen in Figure 11a, became surrounded by bright rims in Figure 11b. Similarly, the newly formed dark holes indicated with an arrow in Figure 11b became surrounded by bright ridges in Figure 11c. This did not happen during annealing of dry $C_{390}H_{782}$ crystals, where thickening proceeds simultaneously with the formation of holes. Annealing at 120 °C initiated the growth of linear cracks (Figure 11e) leading to a gradual disintegration of the crystal, which was completed at 130 °C (Figure 11f).

Height histograms of the images of dry PE crystal recorded during annealing are presented in Figure 12a,b. The graph in Figure 12a shows the crystal thickening at different temperatures, which is related to partial unfolding of the chains. The histograms reveal two peaks, where the smaller thickness, L_1, stays almost constant upon annealing at 115 °C. In contrast, the height of the thickened regions, L_2, gradually increases and the corresponding peak is shifted toward higher values during successive imaging at this temperature. The isothermal evolution can be described in terms of a transition between L_1 and L_2. The area of the thickened regions (area under the L_2 histogram peak) increases at the expense of yet unchanged regions. This process continued after the temperature rise to 120 °C. Further annealing at 120 °C induced a shift of both L_1 and L_2 distances toward higher values that should be explored. An overall view of the evolution of L_1 and L_2 with annealing time is presented in Figure 12b. Similar evolution of long periods has been found in earlier studies of crystal thickening in mats of PE crystals by X-ray diffraction.[3]

Discussion

Although high-resolution AFM imaging of single crystals of ultralong alkane $C_{390}H_{780}$ and PE shows a close resemblance of their structures, the two materials differ quite significantly in their thermal behavior, especially in the case of dry samples. In addition, annealing the $C_{390}H_{782}$ crystals deposited on graphite is accompanied by a flow of material onto the substrate, resulting in the formation of epitaxial layers. These issues are discussed in more detail in the following.

Single-Crystal Morphology. PE vs the Alkane. AFM images reveal many morphological similarities between the lozenge-shaped single crystals of $C_{390}H_{782}$ and PE, such as sector boundaries and central pleats. Nanometer-scale wrinkles found in different sectors of $C_{390}H_{782}$ crystals are oriented along the (530) planes, similar to the larger-scale corrugations appearing in PE single crystals upon flattening.[3] Therefore, we speculate that the wrinkles may also result from the collapse of the alkane crystals upon transfer onto the substrate. In some cases it was found that noncrystallized material precipitates on the wrinkled surface of the $C_{390}H_{782}$ crystals (images not shown here) to form surface features extended along the [530] direction (self-decoration). This prompts us to suggest that solution-grown alkane crystals also have the shape of a hollow pyramid, albeit probably a shallow one since the tilt angle of crystals grown under similar conditions was too small (i.e., less than 10°) to be detectable by SAXS.[16,17]

It is clear that our present AFM study is unable to directly address the issues related to the crystallography of the fold planes and structural origin of various surface features. However, this technique makes it possible to assess the chain conformation through precise height measurements. Thus, the correspondence of the height of the alkane crystals to the length of a straight stem in F5-folded molecules most probably indicates that the possible tilt of the $C_{390}H_{782}$ chain with respect to the lamellar basal plane is minimal.[49] An alternative suggestion that the same crystal height can be explained by tilted chain in the F4 conformation appears less probable because we were able to observe a stepwise chain unfolding sequence on annealing of the dry alkane crystal consistent with F5 (9.9) ⇒ F4 (12.4) ⇒ F3 (16.6) ⇒ F2 (24.9) ⇒ E (49.7 nm) transition sequence. Furthermore, parallel evidence from SAXS and Raman longitudinal acoustic mode spectra confirm the formation of nontilted F5 crystals of $C_{390}H_{782}$ from bulk toluene solution at room temperature.[17] The observed stepwise thickening is in agreement with recent SAXS data recorded during annealing of single-crystal mats of $C_{390}H_{782}$ (ref 16, Figure 49). Regarding the absence of notable chain tilt in as-grown crystals, a study has been carried out recently on a long alkane with deuterated end caps, using IR spectroscopy and SAXS[20] as well as neutron scattering.[55] The study has revealed that the crystals as formed from solution have rough surfaces with high longitudinal disorder of chain ends and folds. Only on annealing at higher temperatures (>90 °C), as the surface becomes smoother, does the necessity arise for chain ends/folds to stagger to alleviate surface overcrowding. This results in chain shear (chain tilt).

Morphological Pathways during the Chain Unfolding. Monitoring the transformations during thermal annealing of $C_{390}H_{782}$ and PE crystals contribute to our knowledge on their structure and thermodynamics. Recently, the formation of hole morphology and local thickening was revealed in AFM images of single PE crystals.[32] The present work substantially broadens the scope of such studies. One of the most interesting findings is the recognition that the morphological transformation in $C_{390}H_{782}$ is strongly dependent on the presence of traces of solvent, which is in line with Geil's suggestion for PE crystals.[3] During annealing of "wet" $C_{390}H_{782}$ crystals, the flat lamellar surface gives way to a rough morphology made up of ribbons with chains in F2 conformation. At 120 °C, this process is completed within several minutes after having been initiated at the crystal edges. We believe that this is the result of the alkane melting/recrystallization, which takes place locally without major changes of the overall single-crystal dimensions. The fact that the surface roughness

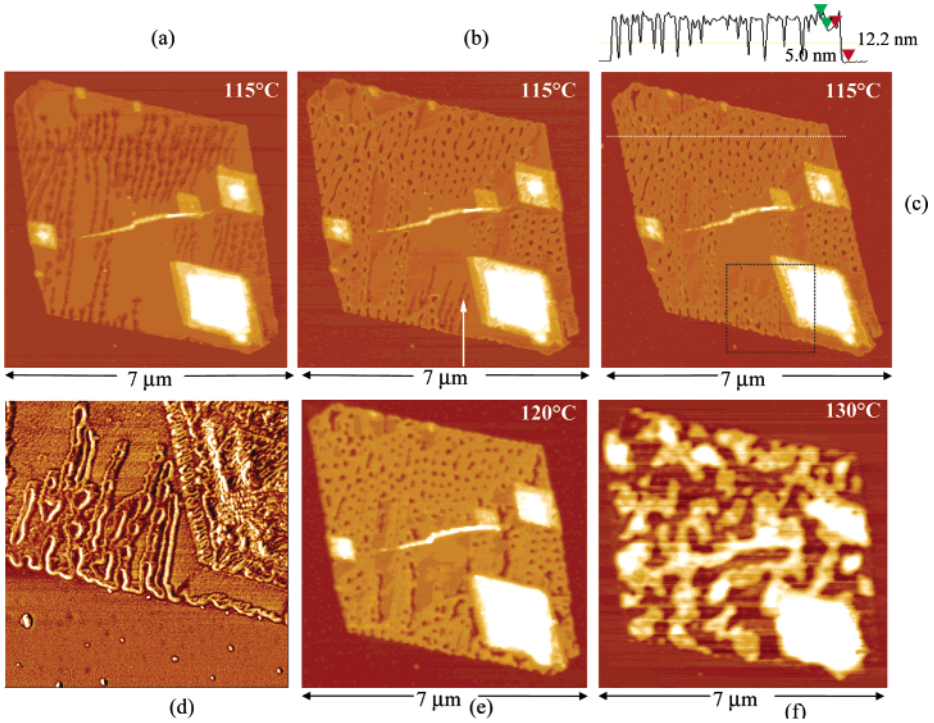

Figure 11. (a−c) Height images of a dry PE crystal on Si substrate at 115 °C. The images are recorded at 10 min intervals. The cross-section profile above the image in part c is measured along the white dotted line. (d) Phase image of a boxed part of the crystal in part c. (e, f) Height images of a dry PE crystal at 120 and 130 °C, respectively.

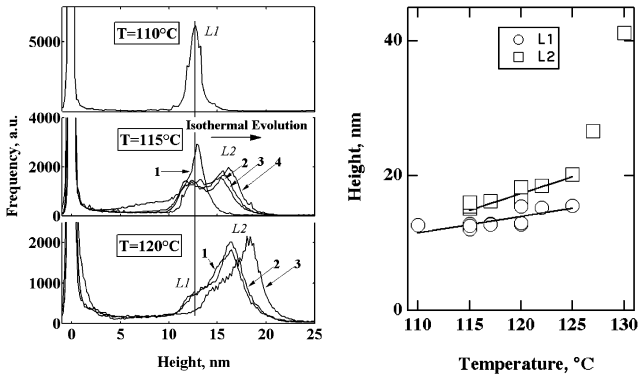

Figure 12. (a) Height histograms computed from the AFM images in Figure 11a−f. Different curves 1, 2, 3, and 4 at 115 °C and 1, 2, and 3 at 120 °C correspond to the images recorded at these temperatures in 10 minutes intervals. L_1 and L_2 represent two characteristic thicknesses of the bimodal height distributions. It is seen that L_1 remains close to the thickness of the initial PE crystal, whereas L_2 reflects the crystal thickening. (b) Temperature dependence of L_1 and L_2.

of the recrystallized crystal is comparable to the thickness of the initial crystal implies that the melting/recrystallization proceeds throughout the whole lamellar thickness. The fact that the edge-on lamellae, which are seen on the surface of the annealed "wet" $C_{390}H_{782}$ crystal, are oriented perpendicular to the expected directions of chain folds in the initial crystal suggests that the melting/recrystallization might be fold-directed. Surface decoration by vapor deposition of linear hydrocarbons is known to produce edge-on ribbons, which are on average oriented normal to the fold plane of PE crystals.[43] Analogous decoration of solution-grown once-folded chain crystals of alkane n-$C_{198}H_{398}$ has been shown to produce perfect sector-specific alignment of the decorating ribbons, thereby confirming the high degree of fold regularity in such crystals.[50] Yet the chevronlike morphology of the annealed "wet" crystals in Figures 2e,f and 4d might suggest a strong involvement of the substrate and/or the fold surface in the formation of lamellar morphology during the recrystallization of "wet" $C_{390}H_{782}$ crystals. The curved shape of individual lamellar ribbons, in which neighboring chains are shifted with respect to each other, reflects their formation in confined geometry. This conclusion is supported by our observations of the chevronlike morphology of layers of ultralong alkanes ($C_{390}H_{782}$ and $C_{242}H_{486}$) deposited on graphite. Therefore, in the case of "wet" crystals of ultralong alkanes deposited on graphite their recrystallization can be initiated at the substrate. This is less probable for "wet" PE crystals on Si and for either PE or the alkanes on other substrates. The related AFM studies are in progress.

We suggest that chain unfolding during annealing of "wet" crystals of both the alkane and PE takes place through solvent-mediated molecular transport. Some constraints, arising from the fact that the chains were packed into crystals during growth, continue to affect the transport process. These looser constraints, associated with the presence of the solvent molecules, mostly affect the paths along which the molecules slip, slither or reptate. Alternatively, chains may diffuse through a crystal by passage of dispiration loops or single chain dislocations,[51,52] as a chain moves from a crystal with short stems to a crystal that contains longer stems and is therefore more stable. All these mechanisms for transporting the chain along its axis can easily carry the chain through the approximately 90° angle between the stem direction in the as-grown crystal and the direction observed in the annealed "wet" crystals. Modeling[53] suggests that there are no special barriers to the passage of dispirations through the 180-degree turn of a fold. It appears that a long stem lying on the substrate and surrounded by solvent molecules is favored in comparison with the shorter stems that make

up the original crystal and is even more favored if the fold surface of the original crystal is present.

Outside the edge of the original crystal (Figure 3a), the azimuthal directions of these thin regions are seen to be approaching randomness. This shows that the fold surface of the original crystal that faced the substrate was still ordered enough to influence the azimuthal direction of the molecules as they moved into and through the solvent-containing region and began to form new crystals, with longer stems, on the substrate. This view is supported by the observation that the direction of these nuclei is generally similar to that observed in the decoration of fold surfaces with paraffin molecules.

AFM images recorded during thermal annealing of dry $C_{390}H_{782}$ crystals on Si have shown the formation of holes surrounded by rims. This morphology reflects local molecular unfolding in the chain direction without the loss of chain orientation. As in the case of "wet" alkane crystals, the thickening proceeds from the crystal edges toward the center. However the elementary event of the chain unfolding includes sub-nm vertical chain translation. This process, operating in the solid state, differs substantially from the melt/recrystallization of "wet" $C_{390}H_{782}$ crystals, which is characterized by chain reorientation.

AFM images reflecting the morphological evolution during annealing of "wet" and dry single crystals of PE are generally consistent with earlier TEM observations and recent AFM studies of these processes.[33] Despite similarities in the thickening mechanisms of "wet" and dry single crystals of PE and the alkane, there are noticeable differences in the behavior of polymer vs its low molecular weight analogue. Annealing of "wet" $C_{390}H_{782}$ crystals leads to a regular pattern of edge-on ordered ribbons, which is in contrast to a less ordered semicrystalline morphology of the melt/recrystallized "wet" PE crystals. Interestingly, in PE the formation of thickened rims does not follow the hole formation immediately. Compared to the alkane, the polymer chains require longer time for local reorganization. It might be that the AFM probe does not "see" this molten surface layer appeared on the surface, and this layer becomes detectable only after ordering which brings material stiffness. We can also suggest that the holes begin to form when free volume, from vacancy-like defects within the crystal or free volume from the pores and channels at the interface between the polymer crystal and the substrate, diffuses[53] to the nascent hole. The diffusion of single chain crystallographic defects, such as a dispiration or a dislocation, from the site of the nascent hole, into the crystal, provides a mechanism that can improve the perfection of the crystal by filling small empty spaces in or under the crystal. After such free volume is eliminated, the thickening process can then build up the rims of the holes, as is observed.

Significant quantities of solvent could be held long enough for the reported observations to be made. It is interesting to note that the height data conclusively eliminate the possibility that enough solvent was trapped under the crystal to create a convex "pillow" or "lens" shape. We suggest that channels and pores, with dimensions normal to the lamella ranging from the diameter of a molecule to something over a nanometer, are abundant. The finite radius of the AFM tip limits determination of the detailed shape of these pores and channels. Otherwise the height images and the plots of height along selected lines that are derived from the same data should provide information about the pores and channels in which solvent might be sequestered when a lamellae, suspended in the solvent in which it grew, was dried onto the substrate.

Epitaxial Order of $C_{390}H_{782}$ on Graphite. Annealing of "wet" crystals of $C_{390}H_{782}$ on graphite is accompanied by a flow of the alkane onto graphite with a formation of epitaxial structures. Figure 4c shows that alkane chains can be transported outside the perimeter of the original crystal, presumably with the help of migrating solvent molecules. These chains crystallize in monolayers on the substrate and can nucleate further growth if additional molecules become available. Studies of polymer epitaxy on different substrates have been known for a long time.[54] Nowadays, they attract increasing attention due to the interest in polymer/oligomer organization in confined geometries and possible applications of such structures as templates for nanometer-scale patterning. In the particular case of epitaxial monolayers of $C_{390}H_{782}$, the alkane forms well-defined ribbons on graphite, with completely extended chains oriented along the substrate surface. The lamellar width in these layers (~43 nm) implies that the chain tilt with respect to the lamellar edge is ~26°. This lamellar order on graphite is preserved for temperatures substantially higher than the "bulk" melting temperature (T_m) of $C_{390}H_{782}$ crystals (T_m = 129 °C for F2 and T_m = 132 °C for E crystals[55]). Before a complete disappearance of the ribbon structure of $C_{390}H_{782}$, which occurs at 185 °C, we observed an increase of the ribbon width from 43 to 48 nm, which is most likely due to decrease in chain tilt. Earlier observations of high-temperature stability of epitaxial layers of $C_{60}H_{122}$ on graphite did not show the presence of any tilt of these molecules in the lamellae.[36] These findings are important for better understanding of self-assembly of alkane chains on graphite and other substrates, which has been extensively studied with scanning tunneling microscopy.[56,57]

Conclusions

AFM study of single crystals of ultralong alkane $C_{390}H_{782}$ and PE with different preparation history provides a wealth of structural data on their structure and morphological transformations accompanying thermal annealing. Ultralong alkanes are generally considered as the most appropriate model for PE, and studies of these compounds can shed light on the mechanisms of polymer crystallization. Indeed, the lozenge-shaped single crystals of $C_{390}H_{782}$ and PE closely resemble each other in such structural details as sectorization, surface pleats and fine surface corrugations. However, their thermal behavior is dissimilar. The structural transitions in $C_{390}H_{782}$ crystals follow the typical oligomer-type integral chain-folding scheme. The chains in the as-prepared crystals adopt the F5 chain conformation with chains practically perpendicular to the lamellar surface. Upon annealing, the alkane crystal undergoes a series of discrete transformations corresponding to stepwise unfolding F5−F4−F3−F2−E. The chain unfolding in PE crystals is a continuous and slower process.

On annealing of "wet" crystals of both the alkane and PE, chain unfolding appears to take place through solvent-mediated melting and recrystallization. This process results in the transformation of parts of the crystal into numerous small crystalline ribbons with the

molecular axis turned on its side. In this process the remaining parts of the crystal preserve the outline of the original crystal. By contrast, annealing of dry crystals of $C_{390}H_{782}$ and PE leads to chain unfolding through longitudinal chain slippage, resulting in the formation of holes and thickened nearby regions.

Melting of "wet" $C_{390}H_{782}$ crystals on graphite is accompanied by spreading of the alkane onto the substrate leading to the formation of a thin epitaxial layer. This is composed of lamellar ribbons with the alkane chains lying parallel to the substrate. The chain tilt detected in these ribbons vanishes during a structural transition occurring prior to the complete melting at 185 °C, i.e., ca. 55 °C above the melting point of the bulk material.

References and Notes

(1) Storcks, K. H. *J. Am. Chem. Soc.* **1938**, *60*, 1753.
(2) Keller, A. *Philos. Mag.* **1957**, *2*, 1171.
(3) Geil, P. H. *Polymer Single Crystals*; John Willey & Sons: New York, 1963.
(4) Bassett, D. C.; Frank, F. C.; Keller, A. *Nature (London)* **1959**, *184*, 810.
(5) Niegisch, W. D.; Swan, P. R. *J. Appl. Phys.* **1960**, *31*, 1906.
(6) Ungar, G.; Putra, E. G. R. *Macromolecules* **2001**, *34*, 5180.
(7) Putra, E. G. R.; Ungar, G. *Macromolecules* **2003**, *36*, 5214.
(8) Reneker, D. H.; Geil, P. H. *J. Appl. Phys.* **1960**, *31*, 1916.
(9) Spells, S. J. In *Characterization of solid polymers*; Spells, S. J., Ed.; Chapman and Hall: London, 1994; p 166.
(10) Keller, A.; O'Connor, A. *Discuss. Faraday Soc.* **1958**, *25*, 114.
(11) Bassett, D. C.; Keller, A. *J. Polym. Sci.* **1959**, *40*, 565.
(12) Statton, W. O.; Geil, P. H. *J. Appl. Polym. Sci.* **1960**, *3*, 357.
(13) Hocquet, S.; Dosiere, M.; Tanzawa, Y.; Koch, M. H. J. *Macromolecules* **2002**, *35*, 5025.
(14) Kovacs, A. J.; Gonthier, A.; Straupe, C. *J. Polym. Sci.: Polym. Symp.* **1975**, *50*, 283.
(15) Bidd, I.; Whiting, M. C. *J. Chem. Soc., Chem. Commun.* **1985**, 543. Brooke, G. M.; Burnett, S.; Mohammed, S.; Proctor, D.; Whiting, M. C. *J. Chem. Soc., Perkin Trans. 1* **1996**, *13*, 1635.
(16) Ungar, G.; Zeng, X. *Chem. Rev.* **2001**, *101*, 4157.
(17) Ungar, G.; Steyny, J.; Keller, A.; Bidd, I.; Whiting, M. C. *Science* **1985**, *229*, 386.
(18) Organ, S. J.; Ungar, G.; Keller, A. *J. Polym. Sci., Part B: Polym. Phys.* **1990** *28*, 2365.
(19) Hobbs, J. K.; Hill, M. J.; Barham, P. J. *Polymer* **2000**, *41*, 8761.
(20) de Silva, D. S. M.; Zeng, X. B.; Ungar, G.; Spells, S. J. *Macromolecules* **2002**, *35*, 7730.
(21) Magonov, S. Visualization of Polymers at Surfaces and Interfaces with Atomic Force Microscopy. Chapter 10 in *Handbook of Surfaces and Interfaces of Materials*; Nalwa, H. S., Ed.; Academic Press: 2001; Vol. 2.
(22) Ivanov, D. A.; Magonov, S. Atomic Force Microscopy Studies of Semicrystalline Polymers at Variable Temperature. In *Polymer Crystallization: Observations, Concepts and Interpretations*; Sommer, J. U., Reiter, G., Eds.; Springer-Verlag: Berlin, 2003; pp 98−129.
(23) Godovsky, Yu. K.; Magonov, S. N. *Langmuir* **2000**, *16*, 3549.
(24) Ivanov, D. A.; Amalou, Z.; Magonov, S. N. *Macromolecules* **2001**, *34*, 8944.
(25) Patil, R.; Kim, S.-J.; Smith, E.; Reneker, D. H.; Weisenhorn, A. L. *Polym. Commun.* **1991**, *64*, 117.
(26) Nakagawa, Y.; Hayashi, H.; Takahagi, T.; Soeda, F.; Ishitani, A.; Toda, A.; Miyaji, H. *Jpn. J. Appl. Phys.* **1994**, *33*, 3771.
(27) Patil, R.; Reneker, D. H. *Polymer* **1994**, *35*, 1909.
(28) Nie, H.-Y.; Motomatsu, M.; Mizutani, W.; Tokumoto, H. *Polymer* **1996**, *37*, 183.
(29) Boyd, R. D.; Badyal, J. P. S. *Adv. Mater.* **1999**, *9*, 895.
(30) Craemer, K.; Wawkuschewski, A.; Domb, A.; Cantow, H.-J.; Magonov, S. N. *Polym. Bull. (Berlin)***1995**, *35*, 457.
(31) Winkel, A. K.; Hobbs, J. K.; Miles, M. J. *Polymer* **2000**, *41*, 8791.
(32) Tian, M.; Loos, J. *J. Polym. Sci. Phys.* **2001**, *39*, 763.
(33) Magonov, S. N.; et al. Manuscript in preparation.
(34) Blundell, D. J.; Keller, A.; Kovacs, A. J. *J. Polym. Sci.* **1966**, *B4*, 481.
(35) Ivanov, D. A.; Daniels, R.; Magonov, S. N. Exploring the High-Temperature AFM and Its Use for Studies Polymers. Application Note published by Digital Instruments/Veeco Metrology Group (February, 2001). URL: http://www.veeco.com/appnotes/AN45_HeatingStage.pdf.
(36) Magonov, S.; Yerina, N. *Langmuir* **2003**, *19*, 504.
(37) Basire, C.; Ivanov, D. A. *Phys. Rev. Lett.* **2000**, *85*, 5587.
(38) Ruland, W. *Colloid Polym. Sci.* **1977**, *255*, 417.
(39) Strobl, G. R.; Schneider, M. *J. Polym. Sci.* **1980**, *18*, 1343.
(40) Press, W. H.; et al. *Numerical Recipes in C, The Art of Scientific Computing*; Plenum Press: New York, 1988.
(41) Further in the text, similar structures whose height is comparable to the diameter of an individual alkane chain will be termed ribbons.
(42) Keller, A. Chain-folded crystallization of polymers from discovery to present day: A personalized journey. In *Sir Charles Frank, An eightieth Birthday Tribute*; Chambers, R. G., Enderby, J. E., Keller, A., Lang, A. R., Steeds, J. W., Eds.; Adam Hilger: Bristol, U.K., 1991.
(43) Wittmann, J. C.; Lotz, B. *J. Polym. Sci., Polym. Phys. Ed.* **1985**, *23*, 205.
(44) Magonov, S.; et al. Thin Layers of $C_{390}H_{782}$. Manuscript in preparation.
(45) Gilbert, E.; Reynolds, P.; White, J. *J. Appl. Crystallogr.* **2000**, *33*, 744.
(46) Hay, I. L.; Keller, A. *J. Mater. Sci.* **1966**, *1*, 41; **1967**, *2*, 538; **1968**, *3*, 646.
(47) Pieszek, W.; Strobl, G. R.; Malzahn, K. *Acta Crystallogr. B* **1974**, *30*, 1278.
(48) Takamizawa, K.; Ogawa, Y.; Oyama, T. *Polym. J.* **1982**, *14*, 441.
(49) The absence of significant chain tilt in collapsed single crystals of $C_{390}H_{782}$ supports earlier data showing that in solution-grown crystals of long alkanes the chains are perpendicular to the lamellar surface.[16] Yet this is at variance with the well-documented fact that PE chains in single crystals are in many instances inclined more significantly, by about 35° with respect to the layer normal, giving rise to (201) basal planes.
(50) Ungar, G.; Organ, S. J. *Polym. Commun.* **1987**, *28*, 232.
(51) Crystallographic Defects in Polymers and What They Do. Reneker, D. H., Mazur, J. In *Computer Simulation of Polymers*; Roe, J.; Prentice Hall: New York, 1990; Chapter 23, pp 332−340.
(52) Defect diffusion models for internal friction processes in polyethylene. Reneker, D. H.; Mazur, J. *J. Phys. (Paris), Colloq. C10, Suppl.* **1985**, *46* (12), C10−C499.
(53) Reneker, D. H.; Mazur, J. *Polymer* **1983**, *24*, 1393.
(54) Wittmann, J. C.; Lotz, B. *Prog. Polym. Sci.* **1990**, *15*, 909.
(55) Ungar, G.; Zeng, X. To be published.
(56) McGonigal, G. C.; Bernhardt, R. H.; Thomson, D. J. *Appl. Phys. Lett.* **1990**, *57*, 28.
(57) Cincotti, S.; Rabe, J. P. *Appl. Phys. Lett.* **1993**, *62*, 3531.

MA0301303